Journal of Solid State Chemistry 183 (2010) 2095–2100

Contents lists available at ScienceDirect

Journal of Solid State Chemistry

journal homepage: www.elsevier.com/locate/jssc

Symmetry of $LaAlO_3$ nanocrystals as a function of crystallite size

P.J. Dereń *, K. Lemański, A. Gągor, A. Watras, M. Małecka, M. Zawadzki

Instytut Niskich Temperatur i Badań Strukturalnych PAN, ul. Okólna 2, Skr. Poczt 1410, 50-950 Wrocław, Poland

ARTICLE INFO

Article history:
Received 26 February 2010
Received in revised form
19 June 2010
Accepted 10 July 2010
Available online 17 July 2010

Keywords:
Nanocrystals
Structure
Perovskites
Phase transition
$LaAlO_3$
Praseodymium
Chromium

ABSTRACT

Properties of $LaAlO_3$ nanocrystallites obtained by the precipitation method, doped with praseodymium and chromium ions were examined by spectroscopic means. Raman spectroscopy, high resolution transmission electron microscopy (HRTEM), X-ray diffraction (XRD) and electronic spectroscopy proved that symmetry of $LaAlO_3$ crystallites depends on their size. At room temperature the smallest obtained crystals (average size $\sim$5 nm) have cubic symmetry, while the largest ones (average size over 110 nm) exhibit rhombohedral symmetry. Possible explanations for this phenomenon are discussed.

1. Introduction

The nanoscale of phosphors involves new scientific issues because most of the emitting ions are located on the surface. Therefore to describe the physical properties of such a system properly, a theoretical approach which works for a bulk sample can no longer be applied. A phosphor already known in the form of a micro-sized powder or in bulk form exhibits new properties when nanosized. For example, it was observed that the refractive index of nanomaterials depends on particle diameter [1] and the effective phonon energy depends on nanocrystalline size [2]. Also, in nanograin form the heat evacuation is impeded and therefore high-power laser excitation produces thermalization of the levels above the excited one and anti-Stokes emission is subsequently observed [3]. The above phenomena are size dependent but are not caused by quantum effects, these being easily observed in semiconductor nanomaterials possessing a narrower band-gap.

The technology of preparation also influences the physical properties of nanosized samples. Many nanocrystals are produced by sol–gel or Pechini methods or so-called wet methods, others by combustion or a mechanochemical one. The wet methods generally need higher annealing temperatures to remove hydroxyl groups. It is also known that the sintering temperature influences grain diameter.

Therefore it is very interesting to investigate nanosized samples and compare their properties with those of bulk samples. This allows determining whether new properties are observed and, particularly, how the preparation procedure influences the properties of the material. Here we focused our attention on the spectroscopic properties of $LaAlO_3$:Pr^{3+} codoped with chromium traces.

Praseodymium-doped crystals are very interesting for photonic applications. First of all, two emitting levels which can be excited in the visible region, i.e. $^3P_0$ and $^1D_2$, are well separated from lower lying ones by energy gaps of about 4000 cm^{-1} and over 6000 cm^{-1}, respectively. Therefore, for most solid hosts nonradiative multiphonon transitions are negligible for them. Secondly, the large number of levels lying below those mentioned above creates several possibilities for red, green and blue emission.

$LaAlO_3$ is a so-called pseudo-cubic perovskite which has a rhombohedral crystal structure with *R*-3*c* space group stable at 300 K and a cubic structure with space group *Pm*-3*m* at temperatures above 800 K [4]. Pr^{3+} ion replaces La^{3+} which occupies the D_3 site symmetry. There are only a few studies on the spectroscopic properties of $LaAlO_3$ monocrystal doped with praseodymium; so far, Allard et al. [5, 6] published some papers in the 1960s and Przemyslaw Deren recently presented a Judd–Ofelt analysis [7]. The multiphonon transition rate of $LaAlO_3$ has been investigated and similarly to the YAP crystal is low [8].

Here we report spectroscopic properties of $LaAlO_3$:Pr^{3+} (1% mol) nanocrystals obtained by the precipitation method. Along with data obtained from electronic spectroscopy the XRD spectra, HRTEM images and Raman spectra are discussed. In the

* Corresponding author.
E-mail address: P.Deren@int.pan.wroc.pl (P.J. Dereń).

0022-4596/$ - see front matter © 2010 Elsevier Inc. All rights reserved.
doi:10.1016/j.jssc.2010.07.015

course of our study we have found that nanocrystalites symmetry depends on their size. At room temperature the smallest obtained (5 nm) have cubic symmetry, the largest ones (above 110 nm) exhibit rhombohedral distortion. This paper associates these properties with morphology and the material preparation procedure. Possible explanations for this phenomenon are discussed.

2. Experimental

Samples were prepared using the precipitation method. The starting materials were aluminum nitrate, lanthanum acetate, and praseodymium chloride. All the salts were dissolved in distilled water and then solvents were added to the precipitant solution. We used ammonia water as the precipitant. After precipitation, the resulting suspension was filtered with a suction filter and washed several times in distilled water. We obtained a white gel, which was dried at 120 ºC for several hours. The gel was divided into seven batches and then annealed for 5 h at temperatures from 800 to 1500 °C. The amount of Pr^{3+} dopant was 1% mol.

Thermogravimetry (TG) together with differential thermal analysis (DTA) showed that all OH^- groups and organic elements were removed from the $LaAlO_3$ samples well below 800 °C (see Fig. 1). Indeed, water was removed at 190 °C and residual organic elements were burnt at about 390 °C.

A Ti:sapphire pulse laser was used as an excitation source. Emission spectra were measured at room temperature, 77 and 10 K; the samples were placed in a closed-cycle helium cryostat produced by APD Cryogenics. To analyze the spectra, a Jobin Yvon THR 1000 monochromator equipped with a CCD camera and photomultiplier was applied. The decay profiles were recorded on a LeCroy digital oscilloscope. The Raman spectra were measured with the Jobin-Yvon Ramanor U-1000 spectrometer equipped with the CCD detector (150–4000 cm^{-1}) and photomultiplier photon counting electronic system (4000–5 cm^{-1}). The 514.5 nm line of the Ar^+ laser (power of ca. 200 mW) was used as an exiting source. The 90° scattering geometry was applied for the measurements. The resolution was 2 cm^{-1}.

Powder diffraction data were collected on X'Pert PRO X-ray diffractometer with PIXcel ultra fast line detector, focusing mirror and Soller slits for Cu$K\alpha$ radiation. The diffraction patterns were collected at room temperature in reflection mode in the range of $20° \le 2\theta \le 140°$ using step scans of 0.026°. The peak profiles were fitted with the pseudo-Voigt function. The widths of the peaks were corrected for instrumental broadening. XRD Flat-Plate Intensity Standard MD 20899 from US Department of Commerce National Institute of Standards and Technology Gainthesburg was used as a standard material. Refinement of the X-ray diffraction patterns for samples prepared at 800 and 1500 °C was done using Rietveld method implemented in Jana2000 program package [9].

Morphology of the samples was investigated by TEM (Philips CM-20 SuperTwin operating at 200 kV and providing 0.25 nm resolution). Besides conventional TEM images, HRTEM images and SAED patterns were recorded. Analysis of TEM and HRTEM images was performed with ImageJ program [10].

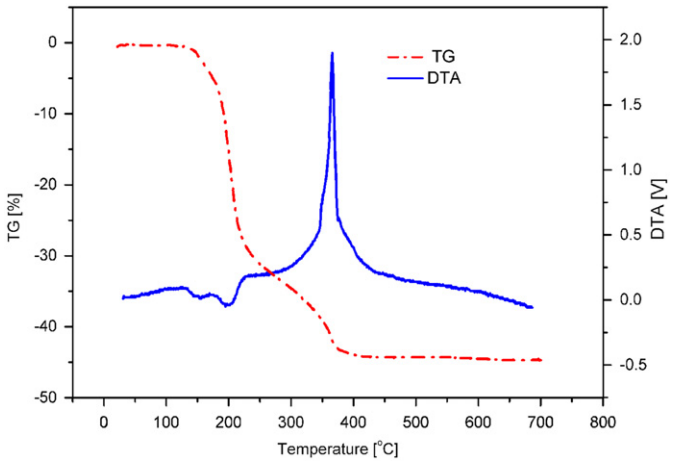

Fig. 1. TG and DTA profiles of the $LaAlO_3$ studied.

3. Results and discussion

The $LaAlO_3$ structure is obtained when the annealing temperature reaches 800 ºC. There were no peaks in the XRD spectra of the samples annealed at lower temperatures (see Supplementary Materials Fig. 10). At higher annealing temperatures, the narrowing of the lines in the XRD spectrum showed an increased degree of crystallization.

The same result gives HRTEM images. At 700 °C there is only an amorphous phase (see Supplementary Material Fig. 11). It was possible to find in TEM images for all annealing temperatures the grains, which diameter ranges from several to several dozens of nanometers. As it was shown in Fig. 2 sample obtained at 1500 °C contains well defined large single crystallites and aggregated fraction of smaller grains that are only several nm in size. Electron diffraction confirms crystallinity of the grains, *d*-spacing shown in Fig. 2 is characteristic for La–O distance that is equal to 2.69 Å in cubic *Pm*-3*m* phase and ranges from 2.54 to 2.82 Å in rhombohedral *R*-3*c* symmetry phase [11].

Because the nanocrystallites are agglomerated the TEM images were insufficient to estimate their average size in a batch. It can be done however from the XRD data. The width of the peak in diffraction pattern has contributions from the instrument optics, micro-strain and contribution from particle size. The first one—instrumental broadening was corrected using standard material, remaining can be separated using Williamson–Hall approach [12]. In the studied systems a splitting of the diffraction peaks that occurs with symmetry decrease from the cubic to the rhombohedral may introduce additional peak broadening. To overcome this effect three peaks that do not show splitting with symmetry change were chosen for calculations (peaks 001, 002 and 004 measured in a wide range of diffraction angle 2Θ: 23.4°, 47.9° and 108.7°, respectively). The Williamson–Hall plots for all samples are presented in Supplementary Materials Fig. 12. Samples annealed at 800 and 900 °C show a slight micro-strain contribution. The maximum value of micro-strain was obtained for 800 °C sample with $\Delta a/a$ ca. 0.05%. The strain is negligible for other samples. The average size of crystallites is burdened with a considerable uncertainty, probably due to the polydispersive character of the measured powders. Even so, exponential growth of average grain size with annealing temperature is observed (see Fig. 3). This indicates an increase of the volume fraction of large crystallites at higher annealing temperatures.

In order to identify the nanocrystals symmetry Rietveld refinement was applied for samples annealed at 800 and 1500 °C. The structure models were taken from Zhao et al. [11]. After the initial refinement of scale, background function, unit cell parameters, profile and asymmetry parameters, the atomic positions were refined. Since refinement of displacement parameters as well as position of oxygen atom led to unrealistic results all these parameters were constrained to values reported by Zhao et al. [11]. No corrections were made for absorption. The Rietveld refinement difference plots for cubic and rhombohedral model for sample annealed at 800 °C are shown in Fig. 4. Final

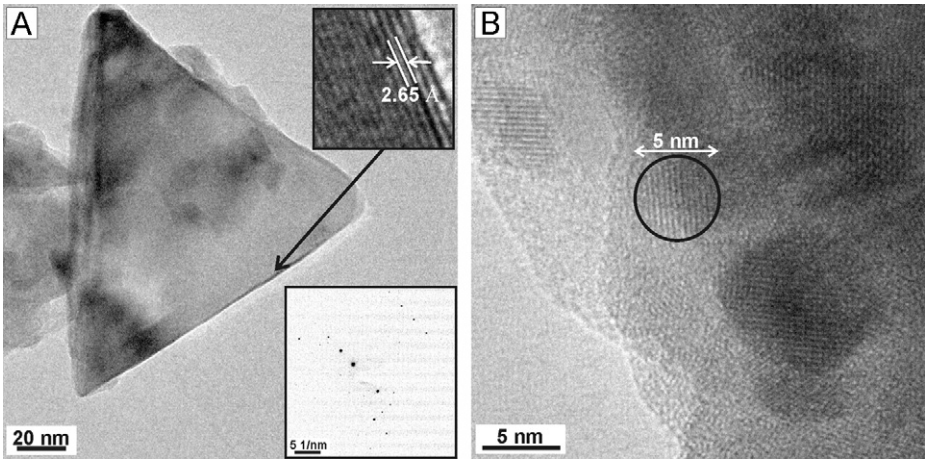

Fig. 2. TEM micrographs of the sample prepared at 1500 °C. The insets show electron diffraction patterns that confirms crystallinity of the grains and magnification with *d*-spacing characteristic for La–O distance.

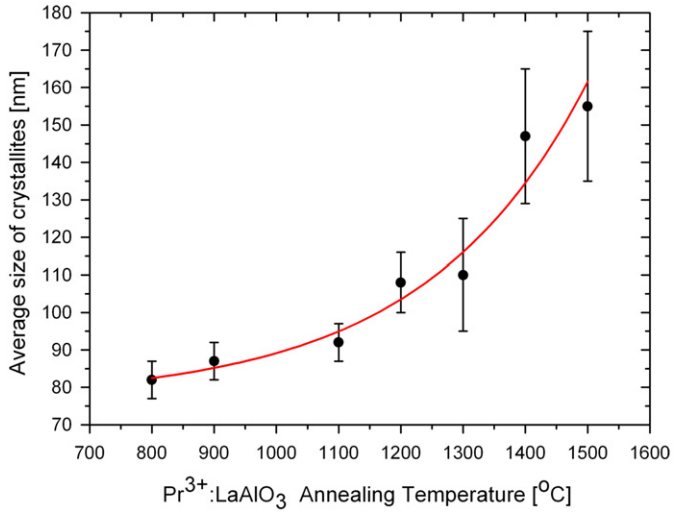

Fig. 3. Average size of crystallites for LAO powders obtained from Williamson–Hall approach.

reliability factors for samples annealed at 800 and 1500 °C are given in Table 1.

The cubic *Pm*-3*m* perovskite structure consists of Al^{3+} ion at (0, 0, 0), La^{3+} at (0.5, 0.5, 0.5) and O^{2-} at (0.5, 0, 0) site. Structural distortion that leads to symmetry decrease from the cubic to the rhombohedral *R*-3*c* is associated with displacement of oxygen atom from (0.5, 0, 0) position and gives only a subtle change in powder diffraction patterns. Usually, size broadening of the peaks precludes distinguishing cubic from distorted phase. As a result the Rietveld refinement performed for 800 °C sample, for which the diffraction peaks are broad, gives good fit for the cubic *Pm*-3*m* as well as the rhombohedral *R*-3*c* symmetry.

Diffractograms of powders annealed above 1200 °C reveal splitting of diffraction peaks (see inset in Fig. 4) characteristic for the distorted rhombohedral phase. However, Rietveld refinement performed for 1500 °C sample in *R*-3*c* symmetry do not give satisfactory results that is probably associated with great dispersion of grain sizes as shown by TEM images and/or fraction of cubic phase that may be present in the measured sample.

The energies of the Pr^{3+} multiplets of the $LaAlO_3$ nanocrystals were obtained from reflectance absorption and emission spectra as well as excitation spectra. As they are the same as those reported in the 1960s [13,14], we will not quote them here. It is worth noting, however, that the full width at half maximum (FWHM) of the $^3P_0$ peak in the excitation spectra decreases by almost 40% with increasing annealing temperature, the same behavior being observed in the emission spectra (see farther).

The emission spectra are characteristic of Pr^{3+} ions. The $^3P_0 \rightarrow {}^3H_6$ transition dominates the spectra, with a maximum at 16326 cm^{-1} (see Fig. 13 in Supplementary Materials), and the second most intense transition at 20368 cm^{-1} was assigned to the $^3P_0 \rightarrow {}^3H_4$ transition. At room temperature, comparable intensities are observed at 15308 cm^{-1} for the $^3P_0 \rightarrow {}^3F_2$ transition and at 13502 cm^{-1} for $^3P_0 \rightarrow {}^3F_4$. It is worth noting that transitions from the $^3P_0$ to the $^3H_5$ and $^3F_3$ levels are present (see peaks at 18387 and 13901 cm^{-1}, respectively) in the emission spectrum although all squared reduced matrix elements are zero for these transitions. Indeed, Judd–Ofelt theory does not work properly for $4f^2$ electrons in this host. The crystal field mixes the praseodymium terms and these transitions turn into allowed ones. At room temperature the emission spectrum becomes richer in lines coming from the $^3P_1$ level. According to the Judd–Ofelt theory, transitions to the $^3H_5$ and $^3H_6$ levels are the strongest and are observed at 18923 and 17105 cm^{-1}, respectively (see Fig. 13 In Supplementary Materials). The lines at 16793 and 16695 cm^{-1}, whose intensities are two orders of magnitude lower than the $^3P_0 \rightarrow {}^3H_4$ transition, were assigned to the $^1D_2 \rightarrow {}^3H_4$ transition. The intensity of the $^1D_2$ emission decreases slightly with increasing annealing temperature.

Careful examination of the emission spectra reveals a very interesting new feature. In general, emission lines are broader for the samples annealed at 800 °C. The FWHM of the $^3P_0$ peak changes from 34 to 19 cm^{-1} with increasing annealing temperature (see Fig. 5). The praseodymium ion sees a different surrounding and this broadening may be associated with different Pr^{3+} sites. This is a situation analogous to that observed in glasses or disordered crystals; the emission line is smeared over large wavelengths. When the crystallization degree increases, the lines become narrower and their intensity increases. We monitored the emission intensity as a function of annealing temperature and the emission intensity indeed increased very rapidly, being two orders of magnitude higher for the 1500 °C sample than for that annealed at 800 °C (see Fig. 5).

To fully understand how spectroscopic properties are influenced by crystalline size, it is necessary to study the emission spectra in detail. Fig. 6 shows spectra in the red region. At 13599 cm^{-1} a line appears which is present only in samples annealed at a temperature higher than 1300 °C. This line was assigned to the so-called *R* line of Cr^{3+} emission. Chromium ions

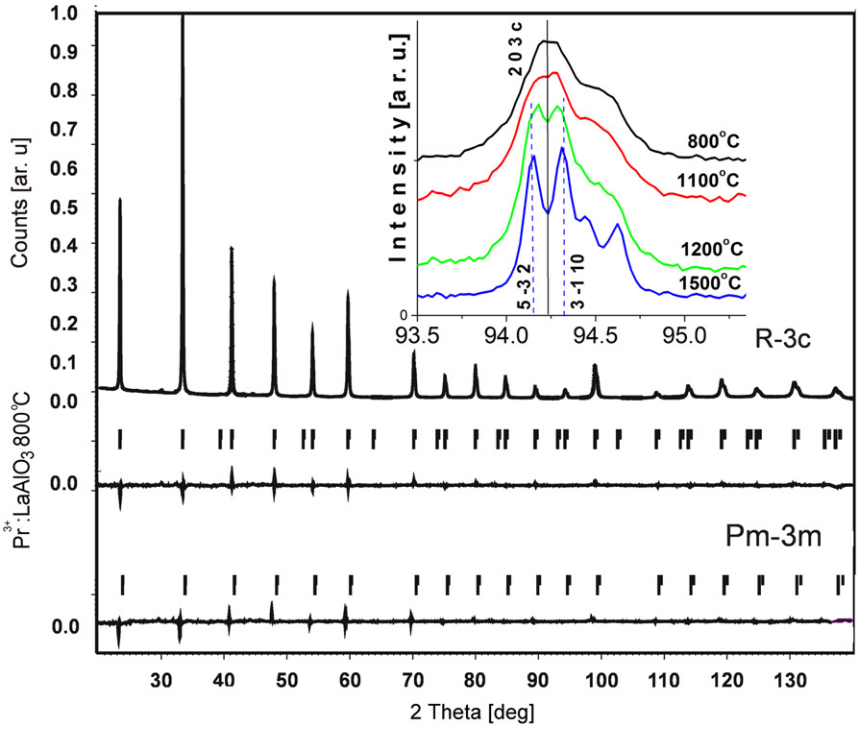

Fig. 4. Rietveld refinement results for Pr^{3+}:$LaAlO_3$ annealed at 800 °C. The upper graph shows the fit between the experimental and calculated patterns for rhombohedral *R*-3*c* symmetry while the lower graphs show the difference between these two patterns for rhombohedral and cubic *Pm*-3*m* symmetry, respectively. The inset shows evolution of 2 0 3 c (cubic) peak for samples annealed at 800, 1100, 1200 and 1500 °C. A distinct splitting that appears above 1200 °C indicates a presence of distorted low symmetry phase. Peaks 5-32 and 3-1 10 are characteristic for rhombohedral phase (the indexation was done in hexagonal unit cell).

Table 1
Final *R*-factors for powders obtained at 800 and 1500 °C from Rietveld refinement.

Sample	800 °C		1500 °C
Phase, lattice parameters	*R*-3*c* a=5.3595(2), c=13.1354(8)	*Pm*-3*m* a=3.79005(3)	*R*-3*c* a=5.3634(7) c=13.111(3)
R_{wp}	0.047	0.045	0.186
R_p	0.035	0.034	0.095
R_F	0.030	0.025	0.085
R_B	0.055	0.048	0.150

$R_p=\Sigma|y_{io}-y_{ic}|/\Sigma y_{io}$; weighted $R_{wp}=[\Sigma w_i(y_{io}-y_{ic})^2/\Sigma w_i y_{io}^2]^{0.5}$; $R_B=\Sigma|I_{ko}-I_{kc}|/\Sigma I_{ko}$; $R_F=\Sigma|F_{ko}-F_{ck}|\Sigma F_{ok}$ where: $y_{io/ic}$ observed/calculated net intensity at the point *i* in the pattern, $I_{ko/kc}$ observed/calculated intensity of *k*th Bragg reflection, *F*-structure factor of *k*th Bragg reflection. Refinements were done with constrained B_{iso} and *x* for oxygen position, parameters were taken from Zhao et al. (B_{iso}: 0.61 Å^2 for La, 0.69 Å^2 for Al and 0.91 Å^2 for O, x=0.5265).

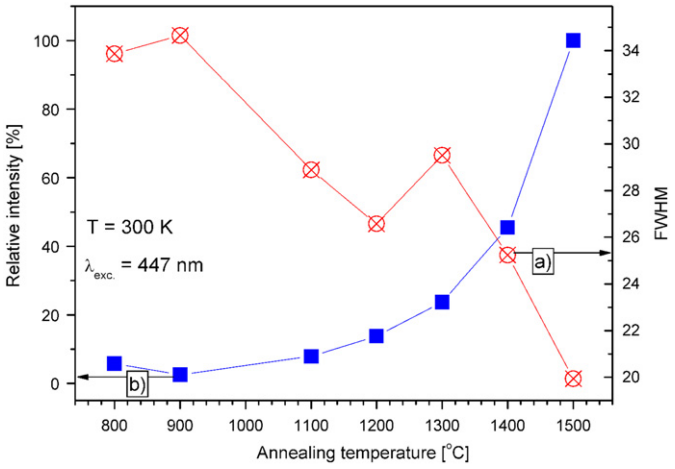

Fig. 5. (a) FWHM of the $^3P_0$ peak and (b) the $^3P_0$ emission intensity as functions of annealing temperature. The lines serve only to guide de eyes.

were introduced to the samples unintentionally with lanthanum and aluminum. The concentration of Cr^{3+} was checked by the inductively coupled plasma (ICP) method and is very small; there is one Cr^{3+} atom for over 21000 aluminum atoms. Since Cr^{3+} is a very good emitter, even traces of chromium are enough to observe the characteristic *R* line. This small amount of chromium added unintentionally appears to be an indicator of the degree of crystallinity and, as we will see later, of crystallite symmetry.

In the emission spectra there are peaks which cannot be assigned to electric dipole (ED) transitions (see Fig. 7). This class of lines could, with some exceptions, be assigned to vibronic transitions. For example, the line at 19579 cm^{-1} is separated from the closest $^3P_0\rightarrow{}^3H_4$ ED 0–0 transition by 794–763 cm^{-1} (the position of the peak increases with increasing annealing temperature). This energy could be assigned to the A_{2g} breathing mode [15]. The peak at 15009 cm^{-1} is separated by 303 cm^{-1} from the $^3P_0\rightarrow{}^3F_2$ ED 0–0 transition and could be assigned to the A_{1u} mode. There are two peaks at 13103 and 13040 cm^{-1} which could be assigned to the E_g mode (469 cm^{-1}) of the $^3P_0\rightarrow{}^3F_4$ ED 0–0 transition. The vanishing of these emission lines with increasing annealing temperature may indicate that the crystallites progressively change their structure and thus local symmetry of the emitting ion.

The lines which were assigned to vibronic transitions are much more intense in the smallest samples obtained at 800–900 °C and their intensity decreases with increasing annealing temperature (see Fig. 7). There are lines which vanish almost completely, for example at 19579, 15009, 13103 and 13040 cm^{-1} (please note that all spectra were normalized to the strongest line of the $^3P_0\rightarrow{}^3H_4$ transition).

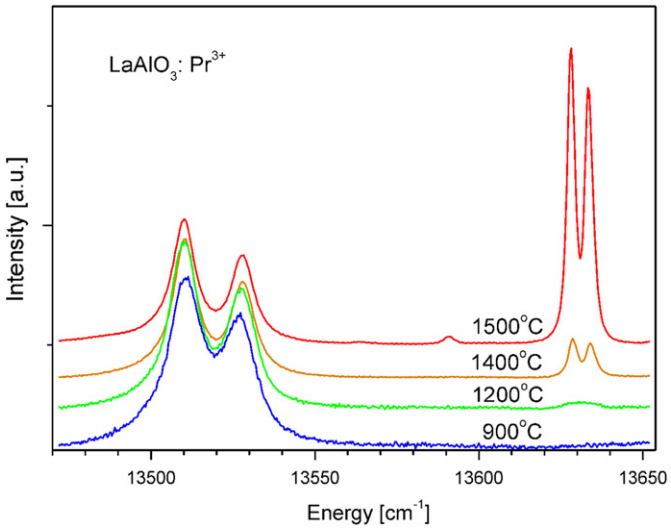

Fig. 6. The 77 K emission spectra of $LaAlO_3:Pr^{3+}$ nanocrystallites as a function of the annealing temperature. Intensities were normalized to the maximum of the $^3P_0 \rightarrow {}^3H_4$ transition.

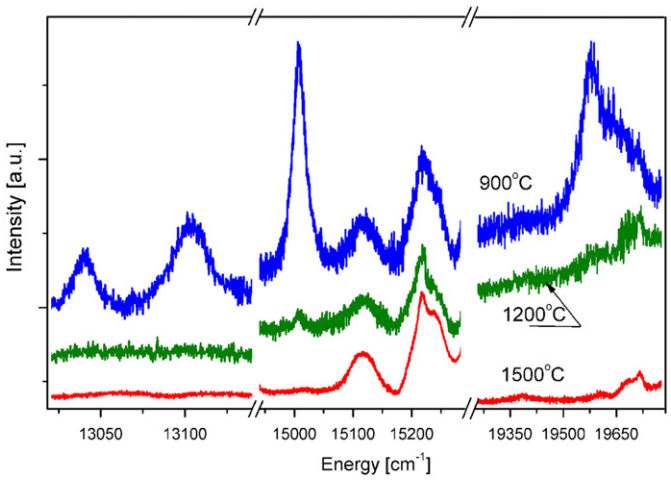

Fig. 7. Vibronic evidences of the $LaAlO_3:Pr^{3+}$ nanocrystallite emission on annealing temperature. The spectra were normalized to the strongest line of the $^3P_0 \rightarrow {}^3H_4$ transition, $T=77$ K, $\lambda_{exc}=447$ nm.

The decay profiles of the $^3P_0$ emission were virtually single exponential both at low and at room temperatures (see Fig. 14 in Supplementary Materials). Decay profile does not depend very much on the measuring temperature; for example, for the sample annealed at 900°C the decay time was 14 and 13 μs at room and at 77 K, respectively. It does not change very much at lower temperature and is 15 μs at 10 K. This indicates a high quantum efficiency for all the samples, showing that even at room temperature, multiphonon nonradiative transitions are negligible in all samples. Here it is worth reminding the reader that all functional groups, such as OH^- and organic ones, have already left the matrix at 450 °C; highly energetic phonons, which are essential in nonradiative transitions are thus absent in the samples.

Although the decay time of the $^3P_0$ emission does not depend on the measuring temperature, it changes very much with annealing temperature, from 13 to 27 μs for samples annealed at 800 and 1300 °C, respectively (see Fig. 8). It should be pointed out that a value of 27 μs was also obtained for $LaAlO_3:Pr^{3+}$ monocrystal and is close to the radiative decay time [7].

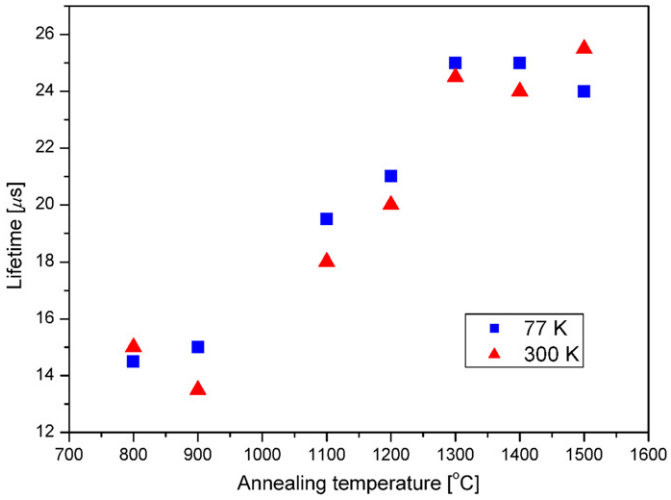

Fig. 8. Decay times of the $^3P_0$ emission in the $LaAlO_3$ nanocrystallites as a function of annealing temperature.

Annealing at a higher temperature does not increase the decay time any further. We were expecting that since the decay time does not change for the samples annealed at temperatures higher than 1300 °C and is almost the radiative decay time, the intensity will not change, either, but it increases constantly (see Fig. 5) and do not reach a plateau even up to 1500 °C. It is an interesting result which could be explained by a better degree of crystallization of the samples; we should also consider changes in the symmetry of praseodymium.

The increased degree of crystallization and changes of local symmetry are very well manifested by the appearance of the strong R line of Cr^{3+}. For cubic $LaAlO_3$ the Cr^{3+} is situated in centrosymmetric site; therefore, no chromium emission is observed. Indeed the R line is invisible in the 800 °C sample, appears for the sample annealed at 1200 °C, and become very intense in the sample annealed at 1500 °C (see Fig. 6). We may conclude that nanocrystals obtained at 800 °C have cubic symmetry and Cr^{3+} is located at center of inversion. When nanocrystallite size increases rhombohedral distortion increases too and as a result the chromium emission intensity increases together with increasing of rhombohedral distortion. Increased rhombohedral distortion influences the Pr^{3+} emission too. Its intensity increases two orders of magnitude and vibronic transition emission lines vanish leaving only pure electronic ones (see Fig. 7).

To find final support of our hypothesis we performed Raman spectra. The number of peaks in Raman spectra depends on crystal symmetry. As Abrashev et al. [15] showed for $LaAlO_3$, the E_g and A_{1g} modes are active. Since there are four E_g and one A_{1g} mode, five peaks are observed for the $LaAlO_3$ structure. The highest observed peak was at 464 cm^{-1} and was assigned to the E_g mode. It has to be stressed that there is no Raman mode active for cubic symmetry. The Raman spectra of all the samples were measured with the same setup and the powders were placed in identical holders and positioned exactly at the same place; therefore they can be compared. Special attention was paid to the 15–300 cm^{-1} region (see Fig. 9). Both the peak intensities and the peak positions depend on the annealing temperature, the most intense being the peaks for the 1500 °C sample. The most prominent peak is observed at 31 cm^{-1}. Peaks are also observed at 117, 153 and 221 cm^{-1}. Abrashev et al. [15] showed that the Raman mode of A_{1g} symmetry at 123 cm^{-1} involves atomic motions that cause rhombohedral distortion, and its position

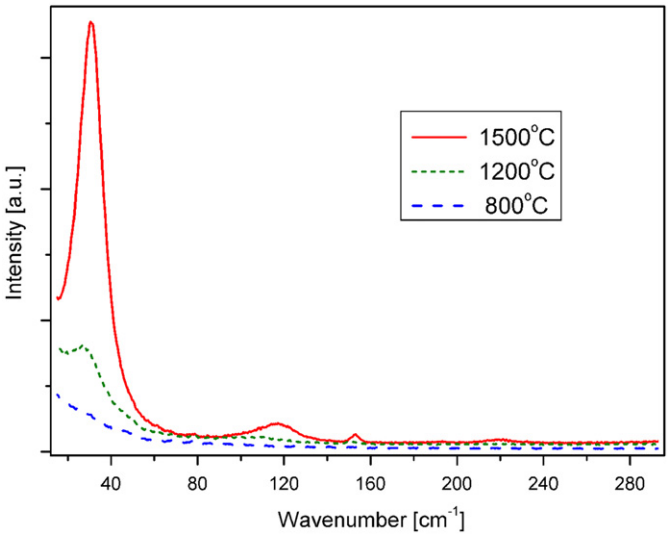

Fig. 9. The 300 K Raman spectra of the $LaAlO_3:Pr^{3+}$ nanocrystallites as a function of annealing temperature excited at 514.5 nm.

could be used as a measure of the degree of the distortion. Indeed the position of this peak changes from 123 cm^{-1} for the bulk crystal to 117 cm^{-1} for the 1500 °C and 108 cm^{-1} for the 1200 °C sample, and the peak vanish for samples annealed at 800–900 °C.

It has to be point up that for the last-mentioned sample there is no peak present in the Raman spectrum. This undoubtedly indicates that with decreasing crystallite size the distortion decreases and eventually vanishes, which is clear evidence that the structure has cubic symmetry in the samples annealed at 800–900 °C. To explain why smaller nanocrystal has higher symmetry let compare surface to volume ratio of an ideal crystal and a nanocrystal. This ratio changes from zero (an ideal crystal has no surface) to considerable value, respectively. At high temperature atoms in $LaAlO_3$ bulk have higher degree of freedom and crystal undergoes phase transition to cubic symmetry. The surface layer of a nanocrystal is relaxed with respect to the bulk and here also atoms having higher degree of freedom attain the cubic symmetry.

4. Conclusions

It was found that the symmetry of $LaAlO_3$ nanocrystals depends on their size and that the electronic spectroscopy is sensitive and versatile method to prove it. To confirm our hypothesis another spectroscopic techniques were applied. High resolution (HR) XRD diffractograms and Raman spectra supplied very strong confirmations of our hypothesis. The samples with larger mean size exhibit in the X-ray diffractograms features characteristic for rhombohedral structure, which are absent in the XRD of samples with smaller mean size. The same is observed in Raman spectra, which exhibits characteristic features for rhombohedral structure only for larger samples.

The HRTEM images show that $LaAlO_3$ nanocrystalites size produced by the precipitation method is ranging from few to dozens of nanometers, but neither TEM images nor the XRD data supply the particle size distribution values. Although we do not have information how the nanocrystalites size is distributed in one batch we can draw from the XRD data the value of their average size and it was proved that it increases with increasing of the annealing temperature.

The importance of presented results is not restricted only to emission properties. Since the rhombohedral phase is of special interest as it is typical for some perovskites exhibiting "colossal" negative magnetoresistance (CMR) we know from this work, that possibility of creation of nanomaterials with well defined rhombohedral distortion appears. Our present aim is to develop a method which gives higher homogeneity of the produced nanocrystals.

Acknowledgments

This work was supported by the Polish Ministry of Science and Higher Education under Grant no. N N507 372335. The authors thank Prof. J. Baran for Raman spectra measurements.

Appendix A. Supplementary material

Supplementary data associated with this article can be found in the online version at doi:10.1016/j.jssc.2010.07.015.

References

[1] R.S. Meltzer, S.P. Feofilov, B. Tissue, H.B. Yuan, Phys. Rev. B 60 (1999) 14012–14015.
[2] H.S. Yang, K.S. Hong, S.P. Feofilov, Brian M. Tissue, R.S. Meltzer, W.M. Dennis, J. Lumin. 83 (1999) 139–145.
[3] W. Stręk, D. Hreniak, A. Bednarkiewicz, P. Mazur, P.J. Dereń, W. Lojkowski, Proc. SPIE 5508 (2004) 238–244.
[4] P.J. Dereń, R. Mahiou, Opt. Mater. 29 (2007) 766–772.
[5] N. Pelletier-Allard, F.M. Brunetiere, J. Phys. 30 (1969) 849.
[6] C. Delsart, N. Pelletier-Allard, J. Phys. C: Solid State Phys. 6 (1973) (1973) 1277.
[7] P.J. Dereń, J. Lumin. 122 (2007) 40–43.
[8] P.J. Dereń, Rachid Mahiou, P. Goldner, Opt. Mater. 31 (2009) 465–469.
[9] V. Petricek, M. Dusek, JANA2000. Structure determination software programs. Institute of Physics, Praha, Czech Republic, 2000.
[10] W.S. Rasband, ImageJ, US National Institutes of Health, Bethesda, Maryland, USA (1997–2005), 〈http://rsb.info.nih.gov/ij〉.
[11] J. Zhao, N.L. Ross, R.J. Angel, J. Phys. Condens. Matter 16 (2004) 8763–8773.
[12] G.K. Williamson, W.H. Hall, Acta Metall. 1 (1953) 22.
[13] M.C. Delsart, M.A. Kastler, C.R. Acad. Sc. Paris 263 (1966) 744.
[14] F.M. Brunetiere, J. Phys. 30 (1969) 839.
[15] M.V. Abrashev, A.P. Litvinchuk, M.N. Iliev, R.L. Meng, V.N. Popov, V.G. Ivanov, R.A. Chakalov, C. Thomsen, Phys. Rev. B 59 (1999) 4146–4153.